scientific reports

Check for updates

OPEN

Longitudinal analysis of brain functional connectivity and its association with clinical assessment in depressed patients using resting state fMRI

Vincent Chin-Hung Chen[1,2], Zi-You Qiu[3], Yuan-Hsiung Tsai[1,4], Gigin Lin[5,6], Yi-Peng Eve Chang[7] & Jun-Cheng Weng[3,6]✉

Suicidal ideation (SI) is an important predictor of suicide attempts, yet SI is difficult to predict. It is also important to understand the associations between network function and SI (or the absence of suicidal ideation, NS) in patients with depression. We recruited 83 participants and divided them into four groups: 25 healthy controls (HCs), 27 depressed patients without suicidal ideation (NS), 18 depressed patients with suicidal ideation (SI), and 13 depressed patients whose SI was converted to NS (improved). All subjects underwent resting-state fMRI at baseline (TP1) and one year later (TP2) after receiving therapy. Patients also underwent four clinical assessments that yielded scale scores. We used the mean amplitude of low-frequency fluctuations (mfALFF) and mean regional homogeneity (mReHo) to compare the function of each brain region at TP1 and TP2. Graph theoretical analysis and network-based statistic analysis were performed to assess changes in connectivity from TP1 to TP2. Multiple regression analysis was also used to examine the association between brain function alterations and clinical assessment changes in each group. Post-treatment, significant functional activity differences were observed: in the cuneus and cingulate for NS; inferior parietal lobule and frontal regions for SI; and parahippocampus and thalamus for the improved group. Increased functional interconnections were noted among frontal, occipital, and temporal lobes. Several connectivity changes correlated with clinical assessment variations (HAM-D, HADS-A, BSS, RRS) across groups, including the caudate, precuneus, and cingulate. We deliberated on the impact of treatment on distinct cerebral regions within the NS and SI cohorts across various conditions. Within the improved group, discernible alterations in brain function following treatment amelioration were identified among the same cohort of individuals, encapsulating modifications in both pathological conditions and cerebral functionality. These findings contribute to our understanding of the neural correlates of depressive disorder and suicidal ideation and highlight the potential impact of therapeutic interventions on brain function in these populations.

Keywords Depressive disorder, Suicidal ideation, Resting-state fMRI, Amplitude of low-frequency fluctuations (ALFF), Regional homogeneity (ReHo)

Depression is a prevalent disorder in the general population, and individuals with severe depression often experience suicidal ideation (SI), and more than 700,000 people die annually because of suicide[1,2]. Suicide is often viewed as a process that involves a range of thoughts and actions progressing from mild to severe forms of suicidality[3]. Research conducted in 17 developed and developing countries demonstrated that approximately

[1]School of Medicine, Chang Gung University, Taoyuan, Taiwan. [2]Tai-An Hospital, Taichung, Taiwan. [3]Department of Medical Imaging and Radiological Sciences, Chang Gung University, No. 259, Wenhua 1st Rd., Guishan Dist, Taoyuan 33302, Taiwan. [4]Department of Diagnostic Radiology, Chang Gung Memorial Hospital, Chiayi, Taiwan. [5]Department of Medical Imaging and Intervention and Institute for Radiological Research, Chang Gung Memorial Hospital at Linkou and Chang Gung University, Taoyuan, Taiwan. [6]Clinical Metabolomics Core Lab, Chang Gung Memorial Hospital at Linkou, Taoyuan, Taiwan. [7]Department of Counseling and Clinical Psychology, Columbia University, New York City, NY, USA. ✉email: jcweng@mail.cgu.edu.tw

9.2% of individuals have experienced suicidal thoughts at some point in their lives[4]. A study conducted in Asia reported that among those with thoughts of suicide, approximately 29% went on to develop a plan, and 32% made an actual suicide attempt[5]. Within a year, approximately one-third of people harboring suicidal thoughts attempt suicide, and approximately 60% of these cases occur within the initial year of experiencing suicidal ideation[4]. Furthermore, roughly two-thirds (66%) of individuals contemplating suicide have disclosed a history of psychiatric disorders, predominantly major depressive disorder (MDD)[6]. Unfortunately, current methods of assessing suicide risk still rely heavily on the experience of clinicians, and many healthcare practitioners are unfamiliar with effective risk assessment. This reliance on self-reports can be problematic, as patients may deny having suicidal thoughts, leading to reduced vigilance even in individuals with a history of suicidal ideation or behavior[3]. The high rates of suicide among patients discharged from care highlight the limitations of current suicide risk assessments. Therefore, it is crucial to develop new and objective methods for evaluating the risk of suicide that do not rely solely on self-reports[3,7].

Several resting-state functional magnetic resonance imaging (fMRI) studies have been conducted in this field. A recent investigation revealed that female individuals diagnosed with MDD and experiencing thoughts of self-harm exhibited markedly greater resting-state functional connectivity between the amygdala and precuneus/cuneus than did those without suicidal thoughts and healthy controls (HCs)[8]. In addition, another study used the Columbia Suicide Severity Rating Scale (C-SSRS) to assess SI in participants who underwent resting-state fMRI at baseline and after 6 months[9]. According to their results, the salience network (SN) exhibited a functional increase within 6 months after suicide ideation in depressed adolescents. Enhanced resting-state connectivity between the right amygdala and the rostral anterior cingulate cortex (ACC), as observed throughout adolescence, was linked to depressive symptoms in adulthood within a large community-based cohort[10]. Furthermore, reductions in connectivity between the subgenual ACC and the dorsomedial prefrontal cortex (dmPFC), posterior cingulate cortex (PCC), middle temporal gyrus, and angular gyrus over a span of 2 years were linked to elevated depressive symptoms during the 2-year follow-up period[11]while developmental increases in amygdala-subgenual ACC connectivity were associated with depression onset within a 2-year follow-up period. These results provided additional information to determine whether the regions and the network influenced depressive disorder and suicidal ideation in longitudinal research.

The present study aimed to examine three research questions. First, we aimed to measure the interaction within the group and between groups. We investigated whether there were any brain functional changes among the SI and without SI (NS) groups or HCs from baseline (Time 1, TP1) to follow-up (Time 2, TP2; after 1 year of therapy) (group-by-time interaction). Second, we investigated the difference between the two time points. We investigated whether there were any brain function alterations between TP1 and TP2 in depressed patients with SI or NS. We also examined patients in the SI group who converted to NS after treatment (the improved group). Third, we investigated whether there was a longitudinal association between brain function alterations and clinical assessment changes in each group. Our previous cross-sectional study showed that depression with or without SI was associated with functional changes in the temporal gyrus and the cuneus[12]. We also investigated the network-based statistic analysis, including the left middle orbitofrontal gyrus, right middle occipital gyrus, and left superior parietal gyrus, and regression in two assessments (HAM-D and HADS-A). The current longitudinal study shares overlapping samples with our previous cross-sectional study, and the findings of both studies demonstrate reproducibility. In the present study, we aimed to identify potential differences via a longitudinal design and verify whether depressed patients who underwent therapy exhibited the same changes as did those in a previous cross-sectional study.

Results

Participants

This study included a total of 83 participants from Chang Gung Memorial Hospital in Chiayi, Taiwan, who underwent medical examinations and agreed to participate in a longitudinal follow-up. Table 1 and Supplementary Fig. S1 show the demographic characteristics of the participants. As shown in the collected data, all our study participants had a follow-up period of at least one year. Given that this study had a longitudinal design, we did not anticipate significant changes in educational attainment over time. Additionally, the results of each clinical assessment almost showed improved outcomes after the treatment. Every score indicated a decrease in TP2, except for the scores originally indicating normal. In the SI group, there was a significant decrease in the BSS score after treatment, but the BSS score at TP2 was still greater than the nonsuicidal ideation criterion. Therefore, the SI group was still diagnosed with suicidal ideation after the treatment. In the improved group, all scores were lower after treatment; patients obviously improved after treatment. While there was a decrease in RRS scores, the change was not significant. The BSS scores in the SI and improved groups indicated that suicidal ideation was strongly correlated with treatment. We used these score differences to detect associations with brain imaging changes after treatment.

Repeated-measures ANCOVA

ANCOVA was used to evaluate whether the means of the HCs, NS patients, or SI patients significantly differed after controlling for the effect of one or more continuous variables, also known as covariates. The ANCOVA included group and time as factors. In the mfALFF map of the comparison between the HC group and the NS group, we observed differences within the frontal lobe, ACC, and PCC (Fig. 1a–d). Additionally, in the mReHo map, we found differences in the frontal lobe, cingulate gyrus, and postcentral gyrus between the HC group and the NS group (Fig. 1e,f).

According to the mfALFF map comparing the HC group and the SI group, there were differences in the putamen, middle frontal gyrus, and ACC (Fig. 1g–i). In the mReHo map, there were differences in the frontal lobe, corpus callosum, and caudate between the HC group and the SI group (Fig. 1j–l).

	HC at TP1 ($n=25$)	HC at TP2 ($n=25$)		NS at TP1 ($n=27$)	NS at TP2 ($n=27$)	
	Mean (SD)	Mean (SD)	*p* value	Mean (SD)	Mean (SD)	*p* value
Age, years	40.08 (10.6)	42.08 (10.9)	< 0.001	45.00 (9.9)	46.63 (10.1)	< 0.001
Gender (F/M)	22/3			13/14		
Education, years	14.24 (3.4)	14.36 (3.3)	0.18	13.67 (3.6)	13.96 (3.8)	0.057
HAMD score	4.48 (5.4)	2.80 (3.7)	0.12	14.96 (5.8)	6.59 (5.5)	< 0.001
HADS-A score	4.48 (4.2)	4.84 (3.9)	0.58	8.03 (4.1)	6.04 (4.8)	0.08
BSS score	0.80 (2.1)	1.12 (3.5)	0.69	1.37 (2.8)	1.48 (3.6)	0.89
RRS score	37.24 (8.8)	34.64 (12.4)	0.28	48.67 (9.8)	42.15 (13.4)	0.02
	SI at TP1 ($n=18$)	SI at TP2 ($n=18$)		Improved at TP1 ($n=13$)	Improved at TP2 ($n=13$)	
	Mean (SD)	Mean (SD)	p value	Mean (SD)	Mean (SD)	p value
Age, years	38.16 (11.7)	39.50 (11.9)	< 0.001	42.15 (13.1)	43.38 (13.0)	< 0.001
Gender	8/10			9/4		
Education, years	12.28 (3.1)	12.55 (3.1)	0.17	14.15 (3.1)	14.31 (2.9)	0.34
HAMD score	17.50 (6.4)	14.44 (5.8)	0.13	15.07 (4.5)	7.85 (5.6)	< 0.001
HADS-A score	11.83 (3.9)	10.39 (4.6)	0.09	11.84 (4.3)	6.31 (4.9)	0.007
BSS score	15.05 (5.9)	9.89 (6.0)	0.004	10.23 (6.2)	4.77 (6.9)	0.028
RRS score	60.61 (12.9)	53.55 (11.0)	0.02	54.46 (10.56)	46.00 (15.6)	0.07

Table 1. Demographic and clinical characteristics of participants at TP1 and TP2. SD, standard deviation; HC, healthy control; NS, without suicidal ideation; SI, with suicidal ideation; Improved: SI converted to NS, HAM-D, Hamilton Depression Rating Scale; HADS, Hospital Anxiety and Depression Scale; BSS, Beck Scale for Suicidal Ideation; RRS, Ruminative Responses Scale; TP1, Time 1, TP2, Time 2.

According to the mfALFF map comparing the NS group and the SI group, there were differences in the inferior frontal lobe (Fig. 1m). In the mReHo map, there were differences in the middle frontal lobe, insula, and temporal lobe between the NS group and the SI group (Fig. 1n–p).

According to the mfALFF map comparing the SI group and the improved group, there were differences in the thalamus and cingulate gyrus (Fig. 1q,r). In the mReHo map, there were differences in the precentral gyrus, postcentral gyrus, and inferior frontal gyrus between the SI group and the improved group (Fig. 1s–u). A summary of the repeated-measures ANCOVA results, including precise brain regions, T scores, and p values, in different groups are shown in Table 2 (corrected p value of all results < 0.05).

Longitudinal paired-sample t tests

The paired-sample t test was used when the data analyzed were in pairs, with each pair consisting of two related measurements or observations. In our study, we compared the brain function of individuals in each group before and after treatment. In the NS group, the mfALFF maps showed a significant decrease in functional activity within the corpus callosum, paracentral lobule, and cingulate gyrus after treatment (Fig. 2a,b). Conversely, there was an increase in functional activity within the PCC, cuneus, and lingual gyrus after treatment (Fig. 2c,d). The mReHo maps showed reduced functional activity within the inferior frontal lobe and insula after treatment (Fig. 2e,f). Additionally, there was a significant increase in functional activity within the cuneus after treatment (Fig. 2g).

In addition, in the SI group and improved group, mfALFF and mReHo also exhibited differences within several brain regions from TP1 to TP2 (Figs. 3 and 4). According to the mfALFF map of the SI group, the inferior parietal lobe exhibited a decrease in functional activity after treatment (Fig. 3a). mfALFF was increased in the middle and superior frontal lobes, the cingulate gyrus, and the middle temporal lobe (Fig. 3b–d). According to the mReHo map of the SI group, the lingual gyrus, calcarine cortex, and fusiform gyrus exhibited decreased mReHo after treatment (Fig. 3e). In contrast, mReHo was greater in the inferior frontal lobe, cingulate gyrus, insula, postcentral gyrus, and superior temporal gyrus after treatment (Fig. 3f–i).

According to the mfALFF map of the improved group, the superior frontal gyrus, fusiform gyrus, and hippocampus exhibited reduced mfALFF after treatment (Fig. 4a–c). mfALFF increased in the precuneus/cuneus, parahippocampus, lingual gyrus, and pre/postcentral gyrus after treatment (Fig. 4d–f). According to the mReHo map of the improved group, the frontal lobe, thalamus, and hippocampus had reduced mReHo after treatment (Fig. 4g–i). In the lingual gyrus, paracentral gyrus, precentral gyrus, postcentral gyrus, parahippocampus, and cuneus, there was increased mReHo after treatment (Fig. 4j–k). A summary of the paired-sample t test results, including the specific brain regions, T scores, and p values, effect size, for the different groups is shown in Table 3 (corrected p value of all results < 0.05).

Graph theoretical and network-based statistic analyses

Graph theoretical analysis was conducted to examine brain network properties, such as global integration and local segregation. Although no significant changes were found in the topological parameters across most groups, the NS group showed near-significant trends. Specifically, at TP1, the global efficiency was higher than at TP2 (p-value = 0.068), suggesting a decrease in global brain network integration over time. Conversely, transitivity

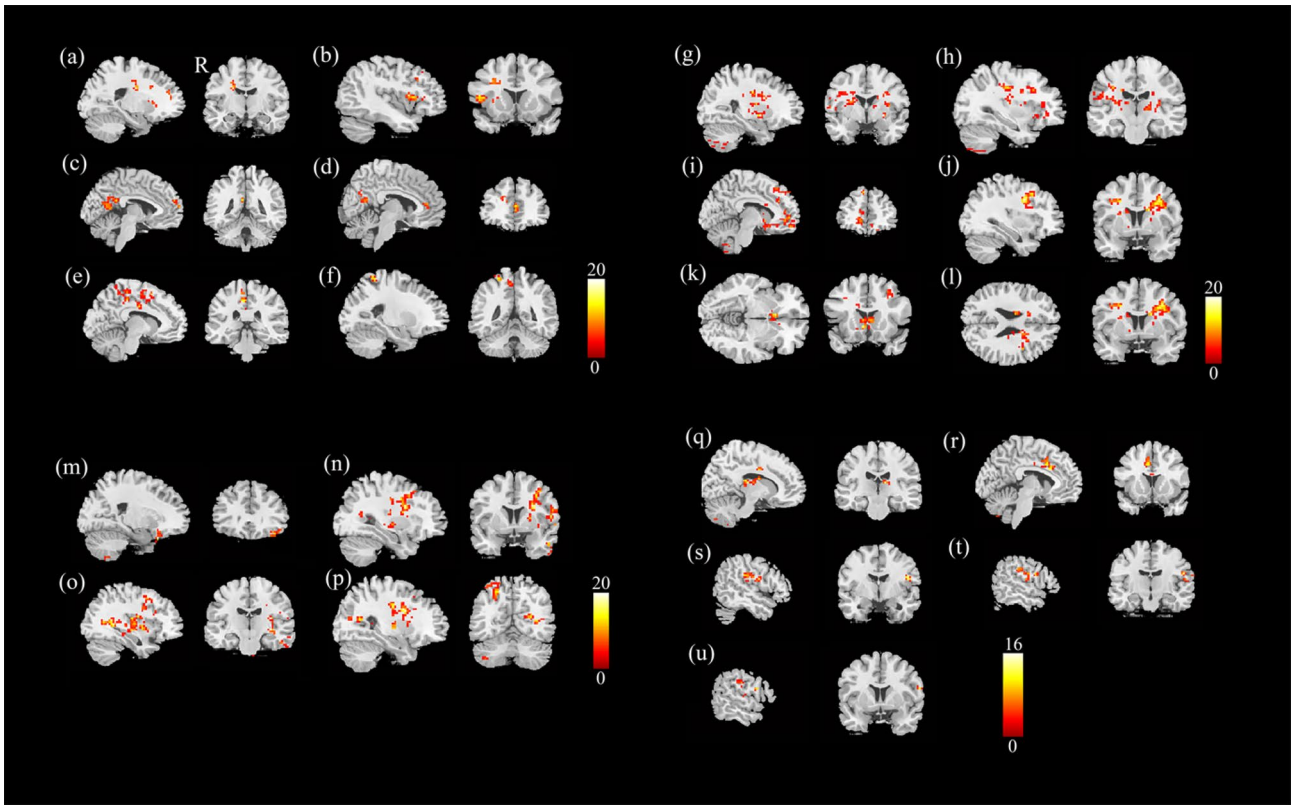


Fig. 1. Repeated-measures ANCOVA results. Comparing the HC group with the NS group, there were differences in the mfALFF in the (**a**,**b**) frontal lobe, (**c**) posterior cingulate, and (**d**) anterior cingulate. There were differences in the mReHo of the (**e**) frontal lobe, cingulate gyrus, and (**f**) postcentral gyrus. Comparing the HC group with the SI group, there were differences in the mfALFF in the (**g**) putamen, (**h**) frontal lobe, and (**i**) anterior cingulate. There were differences in the mReHo of the (**j**) precentral gyrus, (**k**) caudate, and (**l**) corpus callosum. Comparing the NS group with the SI group, the differences in the mfALFF in the (**m**) inferior frontal lobe were detected. There were differences in the mReHo of the (**n**) middle frontal lobe, (**o**) insula, and (**p**) temporal lobe. Comparing the SI group with the improved group, the differences in the mfALFF in the (**q**) thalamus and (**r**) cingulate gyrus were detected. There were differences in the mReHo of the (**s**) precentral gyrus, (**t**) postcentral gyrus, and (**u**) inferior frontal gyrus. The number displayed on the color bar represents their F values (cluster size > 100, corrected p value < 0.05).

was higher at TP2 than at TP1 (p-value = 0.052), indicating an increase in local clustering in brain networks. Additionally, according to the network-based statistic analysis, the NS group exhibited significantly greater interconnections of subnetworks between the bilateral temporal lobe at TP2 than at TP1 (Fig. 5a). We also found that the improved group exhibited significantly greater interconnections of subnetworks among the frontal lobe, occipital lobe, temporal lobe, and putamen at TP2 than at TP1 (Fig. 5b) (corrected p value of all results < 0.05). The NBS results abbreviation are shown in Table 4.

Correlation analysis

In multiple regression analysis, differences in mfALFF/mReHo over time were compared with differences in assessment scores. We found several positive and negative correlations between mfALFF/mReHo alterations and assessment score changes after treatment. There was a negative correlation between the ΔmReHo score in the precentral gyrus and ΔHAMD score in the SI group (Fig. 6a). There were negative correlations of ΔmfALFF and ΔmReHo in the precuneus with ΔHAMD scores in the improved group (Fig. 6b,c). We found a positive correlation between ΔmfALFF in the caudate and ΔHADS-A scores in the improved group (Fig. 6i). We also found a positive correlation between ΔmReHo in the insula and ΔHADS-A scores in the improved group (Fig. 6j). There was a negative correlation between ΔmfALFF and ΔmReHo in the inferior parietal lobe ΔHADS-A scores in the improved group (Fig. 6d,e). There was a positive correlation between ΔmfALFF in the superior temporal gyrus and ΔBSS scores in the SI group (Fig. 6k). There was a negative correlation between ΔmfALFF in the thalamus and ΔRRS score in the SI group (Fig. 6f). There were negative correlations between the ΔmfALFF in the ACC and insula ΔRRS score in the improved group (Fig. 6g,h) (corrected p value of all results < 0.05). Additionally, we generated a scatter plot to visualize the correlation and calculate the correlation coefficient, as shown in Supplementary Fig. S2. All correlation coefficients were greater than 0.4.

HC vs. NS (mfALFF) (for cluster peak)	MNI coordinates (x, y, z)	Peak F score
Right frontal lobe	− 21 − 10 29	16.64
Right anterior cingulate	3 41 11	11.05
Left precentral gyrus	− 42 14 8	10.88
Left posterior cingulate	− 6 − 58 14	6.91
Left medial frontal gyrus	− 12 47 11	13.16
HC vs. NS (mReHo) (for cluster peak)		
Left superior frontal gyrus	− 9 11 56	16.64
Left postcentral gyrus	− 24 − 46 65	16.04
Left cingulate gyrus	− 3 − 13 35	10.01
HC vs. SI (mfALFF) (for cluster peak)		
Right putamen	27 − 1 − 4	25.69
Left medial frontal gyrus	− 9 35 29	14.56
Left anterior cingulate	− 9 47 − 1	12.37
HC vs. SI (mReHo) (for cluster peak)		
Right corpus callosum	15 5 26	23.97
Left caudate	− 6 17 − 4	19.12
Right precentral gyrus	32 6 32	10.01
NS vs. SI (mfALFF) (for cluster peak)		
Right inferior frontal gyrus	48 41 − 13	8.11
NS vs. SI (mReHo) (for cluster peak)		
Right insula	33 − 16 14	15.74
Left superior parietal lobule	− 24 − 61 47	10.96
Right frontal lobe	27 5 26	18.92
Right temporal lobe	36–49 5	13.86
SI vs. improved (mfALFF)(for cluster peak)		
Right thalamus	12–22 14	16.02
Left cingulate gyrus	− 6 14 35	13.04
SI vs. improved (mReHo)(for cluster peak)		
Right precentral gyrus	48 − 4 23	15.7
Right postcentral gyrus	57 − 13 14	8.43
Right inferior frontal gyrus	60 5 20	12.17

Table 2. Repeated-measures ANCOVA results for four kinds of groups (cluster size > 100, corrected $p < 0.05$).

Discussion

Numerous cross-sectional studies have been conducted worldwide to examine depression in the fields of neurology, psychology, etc. In our research, we utilized voxel- and network-based analyses to investigate longitudinal changes during the therapeutic process. We observed differences in functional activity posttreatment, particularly focusing on the improved group. In this cohort, we noted functional decreases in the hippocampus, precuneus, and postcingulate region, suggesting that improvements in depressive conditions may be associated with alterations in default mode network (DMN) function. Interestingly, the parahippocampus exhibited a functional increase, suggesting a potential distinction in DMN involvement between depressive disorder and suicide ideation. Network-based statistic analysis revealed a significant increase in functional interconnections among subnetworks in the frontal lobe, occipital lobe, and temporal lobe posttreatment. Additionally, we identified several functional connectivity alterations in brain areas that correlated with changes in HAM-D, HADS-A, BSS, and RRS scores within each depression group. These alterations involved the caudate, precuneus, superior temporal gyrus, cingulate, and inferior parietal gyrus. According to our results, there are several related points as follows.

Differences in variation among the groups

Repeated-measures ANCOVA was used to compare variance among the groups. We examined the group-by-time interaction in the different groups (HC, NS, and SI groups) at two time points. Significant alterations were observed in the frontal lobe across all types of comparisons. According to the results of our previous cross-sectional study[12]there were significant differences in the cuneus and the middle temporal gyrus between the NS and SI groups. Thus, we can exclude the temporal gyrus and preserve the frontal lobule as a result of the time difference between the NS and SI groups.

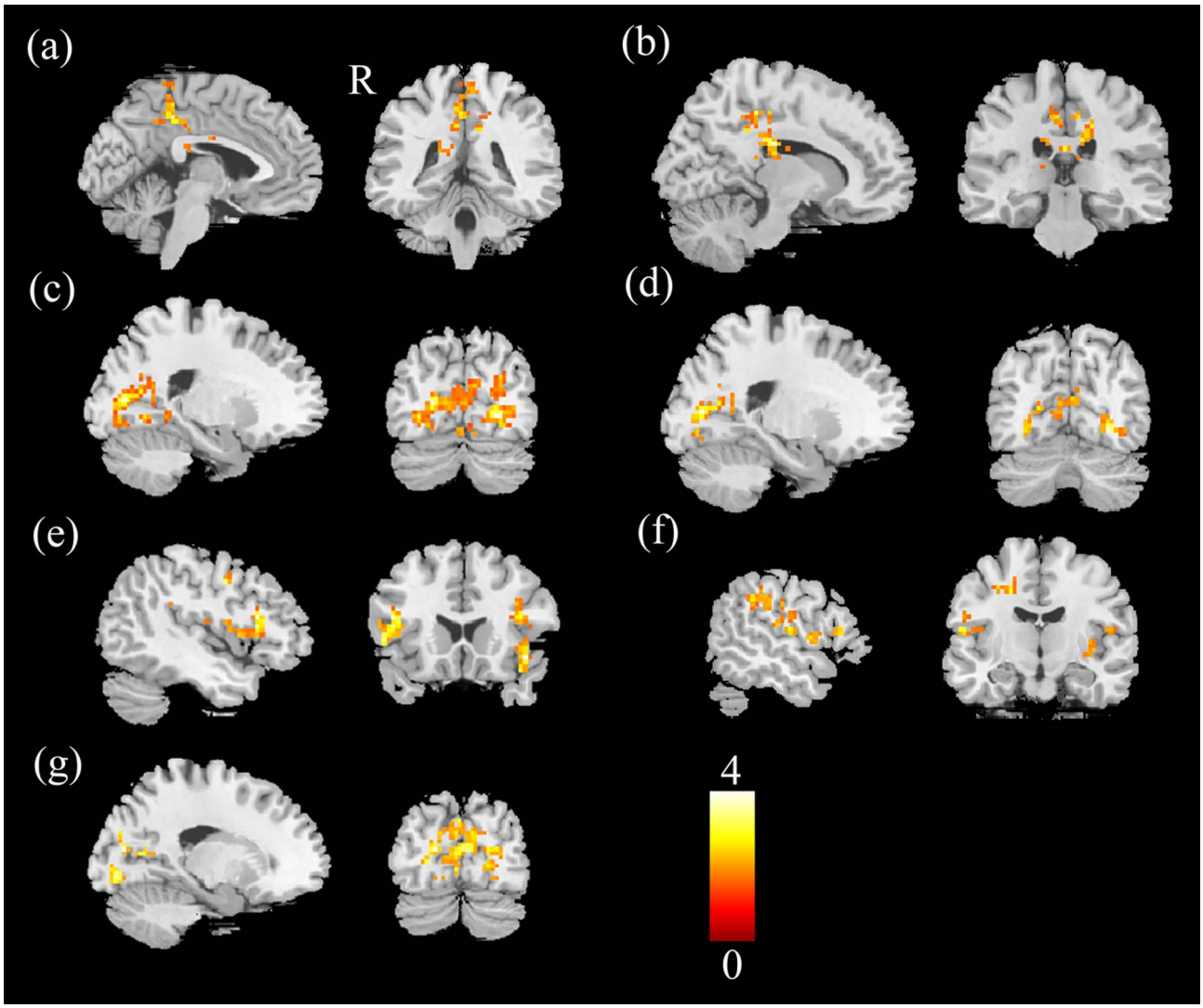


Fig. 2. Paired-sample t test results of changes in the NS group between TP1 and TP2. We found decreased mfALFF in the (**a**) corpus callosum, (**b**) paracentral lobule, and cingulate gyrus after treatment and increased mfALFF in the (**c**) posterior cingulate cortex (PCC), cuneus, and (**d**) lingual gyrus after treatment. We also found reduced mReHo in the (**e**) inferior frontal lobe and (**f**) insula and increased mReHo in the (**g**) cuneus. The number displayed on the color bar represents their T values (cluster size > 100, corrected p value < 0.05).

Furthermore, based on the outcomes of the repeated-measures ANCOVA and subsequent post hoc paired-sample t-test, distinct patterns emerged between the SI group and the improved group across two time points. The ANCOVA comparison highlighted notable differences in the cingulate gyrus regarding mfALFF between the SI and improved groups, along with disparities in the precentral gyrus, postcentral gyrus, and inferior frontal gyrus concerning mReHo. Specifically, the paired t-test within the SI group revealed functional alterations in the cingulate gyrus in mfALFF, alongside multiple changes in the postcentral gyrus and inferior frontal gyrus in mReHo. Additionally, within the improved group, the paired t-test unveiled several findings in the postcentral gyrus and precentral gyrus regarding mReHo. The correlation observed between these statistical analyses suggests that changes in the postcentral gyrus were consistently associated with suicidal ideation, irrespective of whether ideation altered following treatment, while the precentral gyrus exhibited a stronger association with changes in suicidal ideation post-treatment.

Longitudinal differences after treatment

After repeated-measures ANCOVA, post hoc paired-sample t-tests of mfALFF and mReHo values were performed for each depressed group. A previous study showed that there was a strong relationship between depression and the default mode network (DMN)[13]. Similarly, we found changes in several brain regions in the DMN, such as the prefrontal lobe, cingulate cortex, parahippocampus, hippocampus, temporal lobe, and inferior parietal lobe, in each depressed group. As previously mentioned DMN function may increase depressive disorder incidence. In the improved group, functional decreases were observed in the hippocampus and prefrontal lobe, suggesting reduced levels of depression. However, in one region, the parahippocampus region exhibited a functional

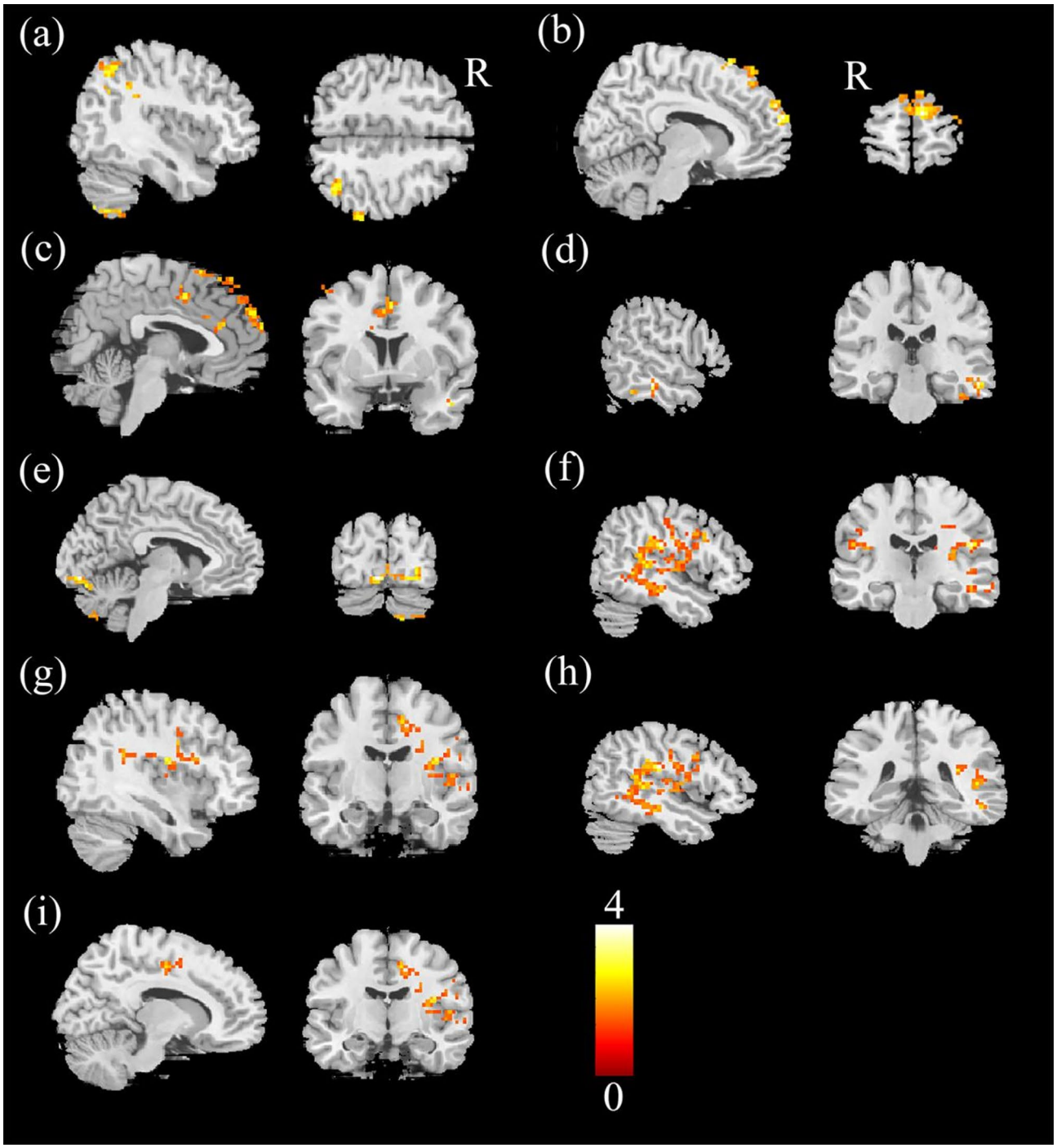


Fig. 3. Paired-sample t test results of changes in the SI group between TP1 and TP2. We found decreased mfALFF in the (**a**) inferior parietal lobe and increased mfALFF in the (**b**) middle lobe, (**c**) superior frontal lobe, (**d**) cingulate gyrus, and middle temporal lobe. We also found reduced mReHo in the (**e**) lingual gyrus, including the calcarine and fusiform gyri, and increased mReHo in the (**f**) inferior frontal lobe, (**g**) cingulate gyrus and insula, (**h**) postcentral gyrus and (**i**) superior temporal gyrus. The number displayed on the color bar represents their T values (cluster size > 100, corrected p value < 0.05).

increase. This may indicate that the DMN is involved only in depressive disorders, not suicide ideation, and that the functional increase in the parahippocampus may be caused by this phenomenon. In addition, there was also a region, the central executive network (CEN), in our study. This region included the middle frontal gyrus, parietal lobule, cingulate cortex, precuneus, temporal lobule, and thalamus. Additionally, in the improved group, several regions, including the middle frontal gyrus and thalamus, exhibited a functional decrease. As indicated after suicide ideation was eliminated, the functions of these areas decreased. Other studies have used

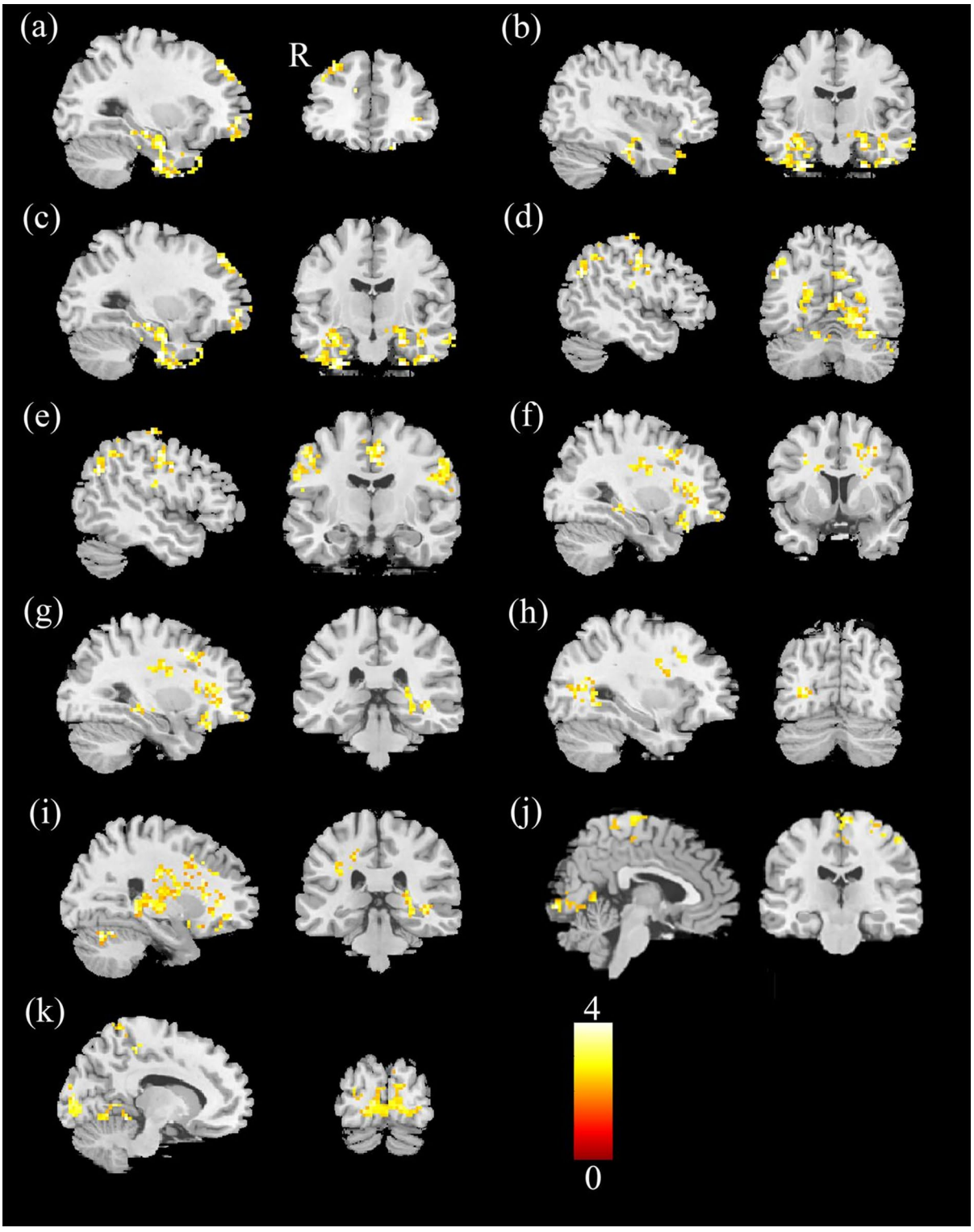


Fig. 4. Paired-sample t test results of changes in the improved group between TP1 and TP2. We found decreased mfALFF in the (**a**) superior frontal gyrus and (**b**) fusiform gyrus and (**c**) hippocampus and increased mfALFF in the (**d**) precuneus/cuneus, (**e**) parahippocampus, (**f**) lingual gyrus and pre/postcentral gyrus. We also found increased mReHo in the (**g**) frontal lobe and (**h**) thalamus and (**i**) hippocampus and decreased mReHo in the (**j**) lingual gyrus and paracentral gyrus, precentral gyrus and postcentral gyrus, and (**k**) parahippocampus and cuneus. The number displayed on the color bar represents their T values (cluster size > 100, corrected p value < 0.05).

NS region (for cluster peak)	MNI coordinates (x, y, z)	Peak T score	Effect size
Right corpus callosum	12 – 22 26	– 4.44	0.43
Left paracentral lobule	– 3 – 37 50	– 2.4	0.18
Left cingulate gyrus	– 3 – 37 44	– 3.62	0.34
Left cuneus	– 13 – 80 12	3.64	0.34
Right lingual gyrus	9–79 – 10	2.49	0.19
Left inferior frontal gyrus	– 44 20 12	– 4.22	0.41
Right insula	42 7 – 5	– 2.92	0.25
Right cuneus	3–73 14	3.41	0.31
SI region (for cluster peak)			
Right inferior parietal lobule	36–64 47	– 2.32	0.24
Left medial frontal gyrus	– 36 35 44	2.94	0.34
Right superior frontal	12 65 20	3.81	0.46
Right cingulate gyrus	9 – 4 47	3.37	0.4
Right middle temporal gyrus	57 – 25 – 16	4.88	0.58
Left lingual gyrus	– 3 – 85 – 10	– 3.84	0.46
Right fusiform	27–85 – 10	– 3.07	0.36
Right inferior frontal gyrus	42 2 32	2.93	0.34
Right cingulate gyrus	12 – 7 47	3.09	0.36
Right Rolandic operculum	39 – 7 17	4.55	0.55
Right postcentral lobule	51 – 22 23	4.06	0.49
Right medial temporal gyrus	45 – 43 2	3.11	0.36
Improved region (for cluster peak)			
Left superior frontal lobule	– 30 41 47	– 2.95	0.42
Right fusiform	42 – 13 – 25	– 3.11	0.45
Left hippocampus	– 27 – 13 – 19	– 2.28	0.3
Right precentral	39 – 19 59	2.02	0.25
Right precuneus	12–67 32	2.83	0.4
Right cuneus	12–88 2	2.43	0.33
Left cuneus	– 12 – 88 2	4.08	0.58
Right parahippocampus	9–43 – 1	2.51	0.34
Right lingual gyrus	6–73 – 4	3.81	0.55
Right postcentral gyrus	42 – 22 53	7.06	0.81
Right superior frontal	9 50 32	– 1.97	0.24
Right middle frontal	33 29 50	– 1.95	0.24
Right thalamus	24–31 2	– 2.00	0.25
Right hippocampus	24–34 – 4	– 2.17	0.28
Left lingual gyrus	– 21 – 58 – 7	2.4	0.32
Right lingual gyrus	18–67 – 7	3.48	0.5
Right paracentral	9–28 53	1.96	0.24
Left precentral	– 39 – 16 41	5.12	0.69
Left postcentral gyrus	– 42 – 25 56	3.33	0.48
Right parahippocampus	21–58 – 7	2.57	0.36
Right cuneus	3–88 2	2.13	0.27
Left cuneus	– 3 – 88 2	2.54	0.35

Table 3. Paired-sample t test results in four kinds of group (cluster size > 100, corrected $p < 0.05$).

rs-fMRI data to assess functional connectivity, focusing on the thalamus and primary somatosensory cortex[14]; increased thalamic functional connectivity was related to decreased cognitive function. The researchers noted that the primary somatosensory cortex is located in the postcentral gyrus and is structurally and functionally connected to the thalamus. This finding supports our finding that the thalamus and postcentral gyrus exhibited significant changes after treatment in the improved group, possibly because increased thalamic functional connectivity was related to decreased cognitive function. A longitudinal study demonstrated brain function changes after aerobic exercise, such as depressive treatment[15]including changes in the fusiform, cingulate, and precuneus regions. These results are similar to our findings in the SI and improved groups, which indicated that the medicine treatment may have cured the same region as exercise treatment. Other researchers used ALFF mapping to analyze MDD patients via a 2 × 2 factorial analysis[16]. Their results were similar to ours in terms of the ALFF in the precentral lobe, postcentral lobe, and lingual gyrus, with alterations after treatment. In this

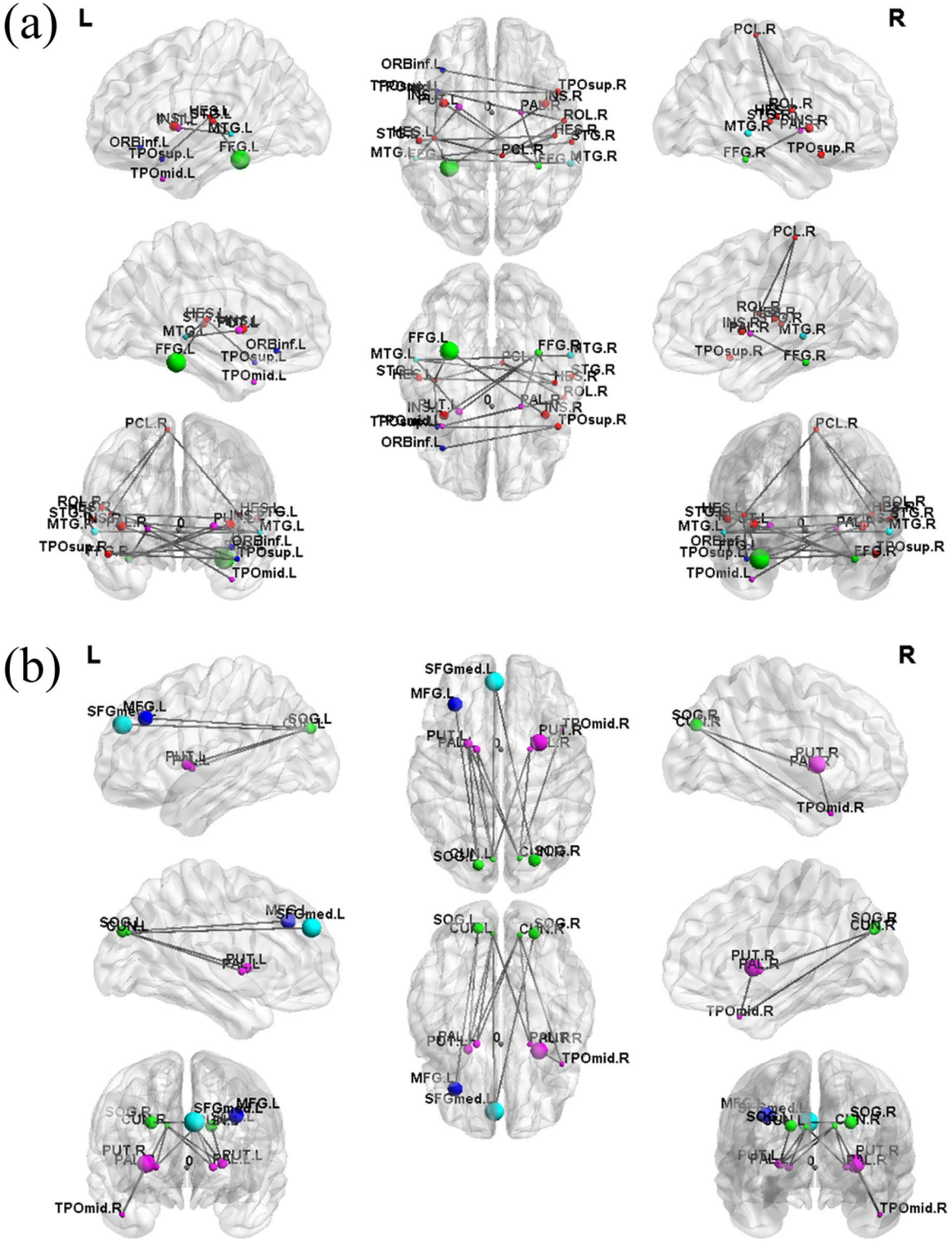


Fig. 5. Network-based statistic analysis comparing the NS group and improved group. (**a**) At TP2, the NS group exhibited significantly greater interconnections between subnetworks of the bilateral temporal lobe than did the TP1 group. (**b**) At TP2, compared with those at TP1, the interconnections of subnetworks among the frontal lobe, occipital lobe, temporal lobe, and putamen were significantly greater in the improved group (corrected $p < 0.05$). NS group: ORBinf.L: left inferior frontal gyrus orbital part; ROL.R: right rolandic operculum; INS.L/R: left and right insula; FFG.L/R: left and right fusiform; PCL.R: right paracentral lobule; PUT.L: left putamen; PAL.R: right pallidum; HES.L/R: left and right heschl gyrus; STG.L/R: left and right superior temporal gyrus; TPOsup.L/R: left and right superior temporal pole; MTG.L/R: left and right middle temporal gyrus; TPOmid.L: left middle temporal pole. Improved group: MFG.L: left middle frontal gyrus; SFGmed.L: left medial superior frontal gyrus; CUN.L/R: left and right cuneus; SOG.L/R: left and right superior occipital gyrus; PUT.L/R: left and right putamen; PAL.L/R: left and right pallidum.

NS group	Left	Right
Left Inferior frontal gyrus, orbital part (ORBinf)	ORBinf.L	
Right Rolandic operculum (ROL)		ROL.R
Insula (INS)	INS.L	INS.R
Fusiform (FFG)	FFG.L	FFG.R
Paracentral lobule (PCL)		PCL.R
Putamen (PUT)	PUT.L	
Pallidum (PAL)		PAL.R
Heschl gyrus (HES)	HES.L	HES.R
Superior temporal gyrus (STG)	STG.L	STG.R
Temporal pole: Superior temporal gyrus (TPOsup)	TPOsup.L	TPOsup.R
Middle temporal gyrus (MTG)	MTG.L	MTG.R
Temporal pole: Middle temporal gyrus (TPOmid)	TPOmid.L	
Improved group		
Left middle frontal gyrus (MFG)	MFG.L	
Left superior frontal gyrus: medial (SFGmed)	SFGmed.L	
Cuneus (CUN)	CUN.L	CUN.R
Superior occipital gyrus (SOG)	SOG.L	SOG.R
Putamen (PUT)	PUT.L	PUT.R
Pallidum (PAL)	PAL.L	PAL.R

Table 4. NBS results abbreviation.

study, they mentioned the main effect in these three regions, which means that childhood trauma did not affect depressive disorder alterations. Therefore, functional changes were found in the postcentral lobe and lingual gyrus. Their results also indicated that childhood trauma had a main effect, significantly decreasing the ALFF of the paracentral lobule.

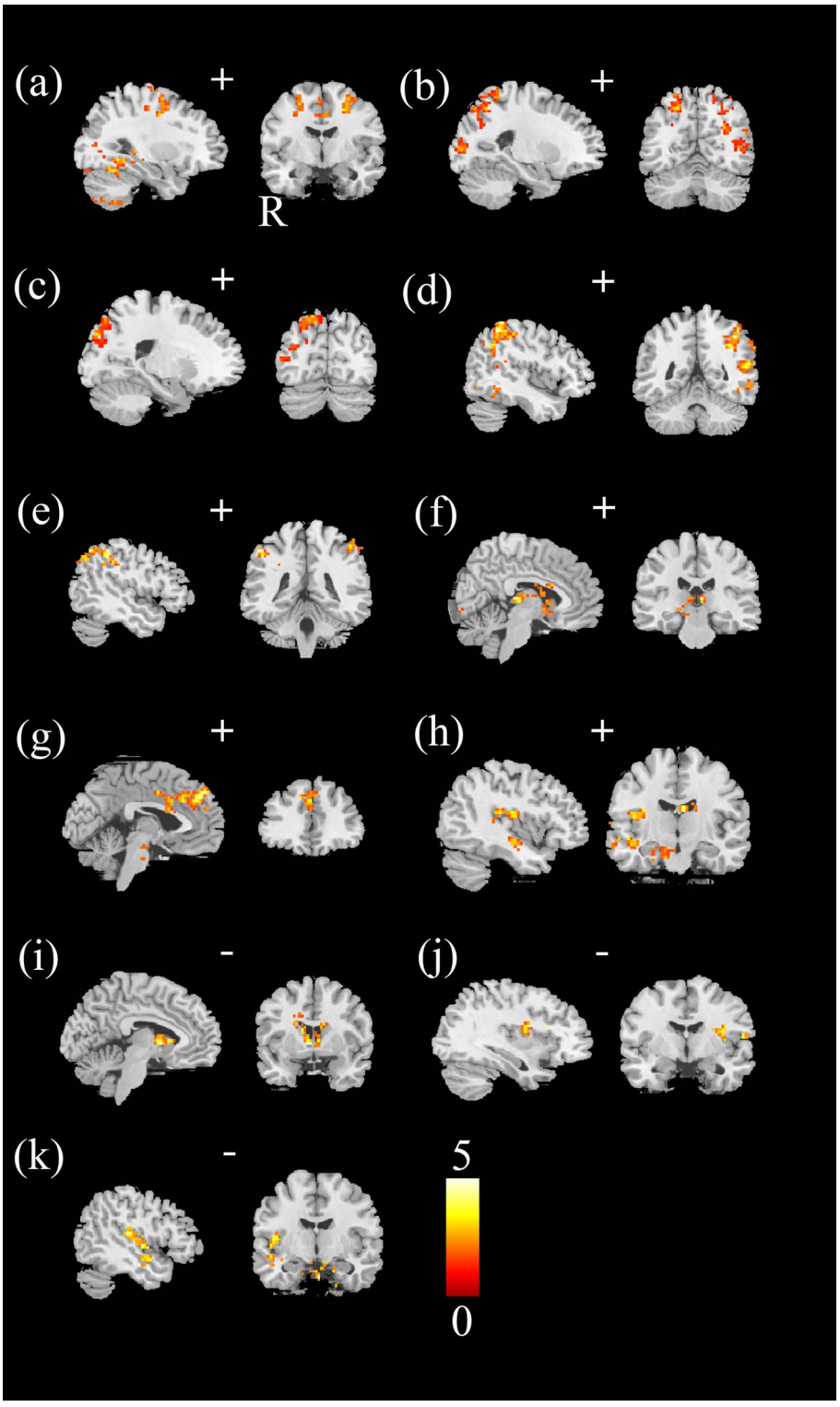
Network analysis results

Although no significant changes were found in the topological parameters across most groups, the NS group showed near-significant trends in global efficiency and transitivity that may reflect unique brain network adaptations in response to treatment. Specifically, at TP1, global efficiency was higher than at TP2 (p-value = 0.068), suggesting a decrease in global brain network integration over time. This decrease could indicate that, as the NS group improved clinically, their brain network reorganized in response to the symptom alleviation. In contrast, transitivity was higher at TP2 than at TP1 (p-value = 0.052), reflecting an increase in local clustering within the brain's network. These changes could suggest that local brain circuits strengthened to maintain or enhance emotional regulation, a process potentially associated with the treatment response in this group. However, it is important to consider that other groups may have still experienced residual suicidal ideation or related symptoms. These lingering symptoms could have influenced their brain network dynamics, possibly leading to different patterns of change compared to the NS group. Despite the lack of traditional statistical significance, the trends in the NS group suggest adaptive changes in brain connectivity in response to symptom improvement. These changes could reflect a neuroplastic response to the reduction of suicidal ideation, which may not have been fully captured in other groups still affected by such symptoms.

Figure 5a shows greater connectivity between the bilateral temporal regions after treatment in the NS group. As shown in Fig. 5b, the improved group had greater connectivity among the frontal lobe, occipital lobe, temporal lobe, and putamen. This result indicated that in the NS and improved groups, several brain regions exhibited increased connectivity after treatment. A previous longitudinal study on suicidal ideation revealed that increases in SN density within two time points were associated with suicidal ideation in the SI group[9]. However, in our study, there were no significant differences in expression in our SI group; instead, there were strong associations with the DMN in the NS and improved groups. We can hypothesize that this change would influence the DMN after treating SI with NS or NS itself. A summary figure is presented in Fig. 7.

Relationships between voxel-based analysis and network-based analysis

Combined with the voxel- and network-based results, there were several relationships among them. In improved emotional regulation and memory: Patients with depression often face challenges in emotional regulation and memory. The increased functionality in areas related to emotional and memory processing (such as the parahippocampus and insula) may signify adjustments in these aspects due to treatment. Improving the functionality of these regions and enhancing their connectivity may contribute to better emotional and memory processing, potentially positively impacting the symptoms of depression. In enhanced cognitive control and executive function, the involvement of the inferior frontal gyrus: orbital region may indicate positive effects of treatment on cognitive control and executive functions. This could aid patients in handling negative cognitions and executing tasks effectively. Improvements in these cognitive functions may help alleviate symptoms of depression, particularly those associated with thinking and cognitive processes. In the integration of perception



and motor information, the increased functionality and connectivity in regions related to perception and motor control (such as the pre/postcentral gyrus and paracentral lobule) may be linked to the goal of improving perceptual–motor coordination and positive engagement in physical activities during treatment.

The improved group may experience a positive impact on patients' body perception and motor performance, contributing to therapeutic effects on depression. In the improved group, voxel-based results indicated a decrease in functional activity in the frontal region and an increase in the cuneus located in the posterior lobe posttreatment. Additionally, network-based results revealed increased connectivity between frontal and occipital regions. As a result, frontal areas, including the superior frontal medial region and middle frontal gyrus, may be implicated in higher-order cognition and motor control[17]. Simultaneously, occipital areas, such as the superior occipital gyrus, are associated with visual processing[18]. In our perspective, the heightened connectivity may

◂**Fig. 6**. Assessments' correlations according to multiple regression analysis. In the SI group, there was a negative correlation between the ΔmReHo and ΔHAMD scores in the (**a**) precentral gyrus. In the improved group, regarding the relationships of ΔmfALFF/ΔmReHo and ΔHAMD scores, there were negative correlations in the (**b**,**c**) precuneus. In the improved group, there was a negative correlation between the ΔmfALFF/ΔmReHo and ΔHADS-A scores in the (**d**,**e**) inferior parietal lobe. In the SI group, regarding the relationship between ΔmfALFF and ΔRRS score, there was a negative correlation in the (**f**) thalamus. In the improved group, there were negative correlations in the (**g**) anterior cingulate and (**h**) insula. In the improved group, regarding the relationship between ΔmfALFF and ΔHADS-A score, there was a positive correlation in the (**i**) caudate. Regarding the relationship between ΔmReHo and ΔHADS-A score, there was a positive correlation in the (**j**) insula in the improved group. (**k**) In the SI group, regarding the relationship between ΔmfALFF and ΔBSS score, there was a positive correlation in the superior temporal gyrus. The number displayed on the color bar represents their T values (absolute value, direction shown as ± and can also be found in supplementary scatter plots, cluster size > 100, corrected p value < 0.05).

	Brain regions	Function
a	Parahippocampus, Insula	Emotional regulation and memory processing
b	Inferior frontal gyrus (orbital region)	Cognitive control and executive function
c	Precentral gyrus, Postcentral gyrus, Paracentral lobule	Perception and motor control
d	Superior frontal medial region, Middle frontal gyrus, Superior occipital gyrus, Cuneus	Visual processing and visuomotor integration

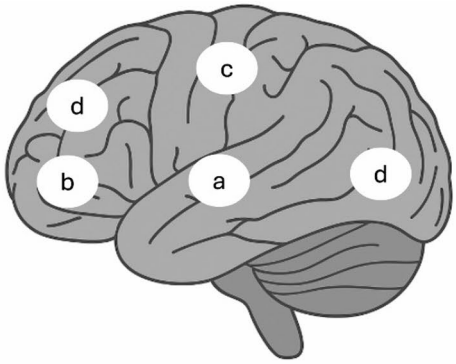


Fig. 7. The summary figure of the relationships between voxel-based analysis and network-based analysis. This figure summarizes the relationships between brain regions and their associated functions based on voxel-based and network-based analysis results. (**a**) Parahippocampus and insula are linked to emotional regulation and memory processing. (**b**) Inferior frontal gyrus (orbital region) is associated with cognitive control and executive function. (**c**) Precentral, postcentral gyri, and paracentral lobule are involved in perception and motor control. (**d**) Superior frontal medial region, middle frontal gyrus, superior occipital gyrus, and cuneus are related to visual processing and visuomotor integration.

reflect tighter integration between the perception and motor control systems post-treatment, facilitating more coordinated visual-motor behaviors.

Association between functional alterations and clinical assessment changes

Regarding the multiple regression analysis of the relationship between clinical assessment changes and functional mapping alterations, our results are similar to those of previous research. In the improved group, insula function was positively correlated with HADS-A scores but negatively correlated with RRS scores. In addition to the changes in brain function associated with differences in scale scores in the aforementioned brain regions, we found that in the SI group, the mReHo of the precentral lobe was negatively correlated with HAMD scores. In addition, in the improved group, the mfALFF and mReHo of the precuneus were negatively correlated with HAMD scores. In the improved group, HADS-A scores were positively correlated with the mfALFF of the caudate but negatively correlated with the mfALFF of the inferior parietal lobe. In the literature, many fMRI studies have reported that patients with general anxiety disorder exhibit elevated insula activation during increased emotional processing[19]. Another fMRI study showed that after 8 weeks of treatment with nefazodone, both remitted and partially improved social anxiety were associated with increased regional cerebral blood flow (rCBF) in the inferior parietal cortex[20]. In the SI group, the mfALFF in the superior temporal lobe was positively associated with the BSS score. The mfALFF in the thalamus was negatively correlated with the RRS score in the SI group; however, in the improved group, the mfALFF in the ACC was negatively correlated with the RRS score. Other fMRI studies have shown correlations with rumination; rumination was strongly related to ACC activity[21]. They found greater ACC activation in the MDDs than in the HCs during different assessments. Moreover, the thalamus exhibited high connectivity with the cingulate cortex to transmit the signal. Thus, we concluded that higher ACC and thalamus activity are associated with lower levels of rumination in the SI and improved groups. According to the above multiple regression analysis, we assessed additional underlying depressive disorder symptoms through different assessments.

Correlation analysis

Although the correlation coefficients between brain activity changes (mfALFF/mReHo) and clinical assessment scores were statistically significant (corrected $p < 0.05$), most were moderate ($r > 0.4$). These moderate correlations

nevertheless suggest meaningful associations that may reflect underlying neural mechanisms of symptom improvement. For example, decreased mReHo in the precentral gyrus correlated with reductions in depression severity in the SI group, potentially reflecting improved motor and cognitive control, which are often disrupted in depression with suicidal ideation[22]. In the precuneus, decreased mfALFF and mReHo were associated with reduced depression scores in the improved group. Since the precuneus is involved in self-referential processing and rumination, these findings may reflect decreased maladaptive self-focus as symptoms improve[23].

Clinically, these associations suggest that changes in specific brain regions may underlie the alleviation or persistence of emotional and cognitive symptoms in depression. While the correlations are not strong enough for diagnostic use, they highlight potential biomarkers of treatment response. Future studies could build on these findings by examining whether these neural changes precede clinical improvements or emerge as a result of them, which would clarify their utility in prognosis and treatment monitoring.

Comparison with a previous cross-sectional study

The majority of studies primarily utilize cross-sectional designs[24]and a cross-sectional study involves a comparison of two independent samples[12]. One of the main advantages of cross-sectional studies is their relatively quick and cost-effective nature, as they do not require long-term follow-up. They are also useful for generating hypotheses and providing a snapshot of the current state of a population or phenomenon. However, they have several limitations, such as an inability to infer causality and susceptibility to cohort effects, where observed differences may be due to generational variations rather than actual changes over time. Thus, compared with the previous cross-sectional study, the present longitudinal study yielded findings that provide more insight into causal relationships. Furthermore, our results are consistent with those of our previous study, which compared NS with SI. A voxel-based analysis study reported similar results in the cuneus as in our improved group. Therefore, regardless of the time difference or group difference, there was high activation in the cuneus in the NS group. According to the other statistical methods, multiple regression, graph theoretical analysis, and network-based statistic analysis, there were no correlations with the cross-sectional study. We only observed increased connections in the cuneus between the two regions. However, since the connected brain regions differ, we cannot have noted that there were similarities between the results of the two studies. It is obvious that the time factor between different groups and different studies indeed produced different results, and the cuneus may have had underlying information related to SI and NS.

Limitations

Limitations of the present study should also be mentioned. First, the sample size was limited, especially in the improved group, due to the difficulty of recruiting participants who initially had suicidal ideation and completed follow-up. This subgroup represents a clinically important but relatively uncommon trajectory, making it hard to collect larger numbers. Second, the HC group consisted mostly of female participants. This gender imbalance may affect the generalizability and interpretation of the results. Future studies should consider including more male participants to enhance the representativeness and reliability of the findings. Third, regarding the four clinical assessments used in the present study, many factors may influence participants' responses, such as their current mood or honesty. Fourth, we did not consider that some patients may have experienced menopause between TP1 and TP2. Fifth, for comorbidities, we controlled for anxiety severity but not all comorbidities, such as personality disorders. Sixth, to mitigate the influence of antidepressant usage, we selected a one-year follow-up sample in which participants used similar antidepressant medications at both baseline and endpoint. Nevertheless, the concurrent use of other psychotropic medications, including benzodiazepines and antipsychotics, was not accounted for, which should be acknowledged as a potential limitation of this research. Finally, we did not account for the effect of psychotherapy.

Conclusions

This longitudinal study used voxel- and network-based analyses to investigate changes in brain function during depression treatment with three trajectories of SI at two time points. Significant alterations were found in the frontal lobe across all groups, with specific differences between the nonsuicidal (NS) and suicidal ideation (SI) groups. Our voxel- based findings highlight significant functional alterations in the DMN and CEN across depressed groups, particularly in regions such as the prefrontal lobe, hippocampus, parahippocampus, thalamus, and middle frontal gyrus. Functional decreases in the hippocampus and prefrontal lobe in the improved group suggest reduced depression severity, while increased parahippocampal activity may indicate its specific involvement in depression rather than suicidal ideation. Network analysis revealed enhanced connectivity in specific brain regions, suggesting positive treatment effects on emotional regulation, memory, cognitive control, and perceptual-motor coordination. Our multiple regression analysis reveals significant associations between clinical assessment changes and functional alterations in specific brain regions (e.g., the insula and precentral gyrus). These findings highlight the critical role of these regions in the pathophysiology of depression, particularly in relation to symptoms such as anxiety, rumination, and suicidal ideation. Our results further emphasize the potential of brain functional markers in assessing depressive symptoms and treatment outcomes. Our longitudinal approach provided a more detailed understanding than cross-sectional studies, emphasizing the dynamic changes in treatment effects on brain function in patients with depressive disorders. In the future, machine learning or deep learning could be included to increase the ease and accuracy of diagnosis.

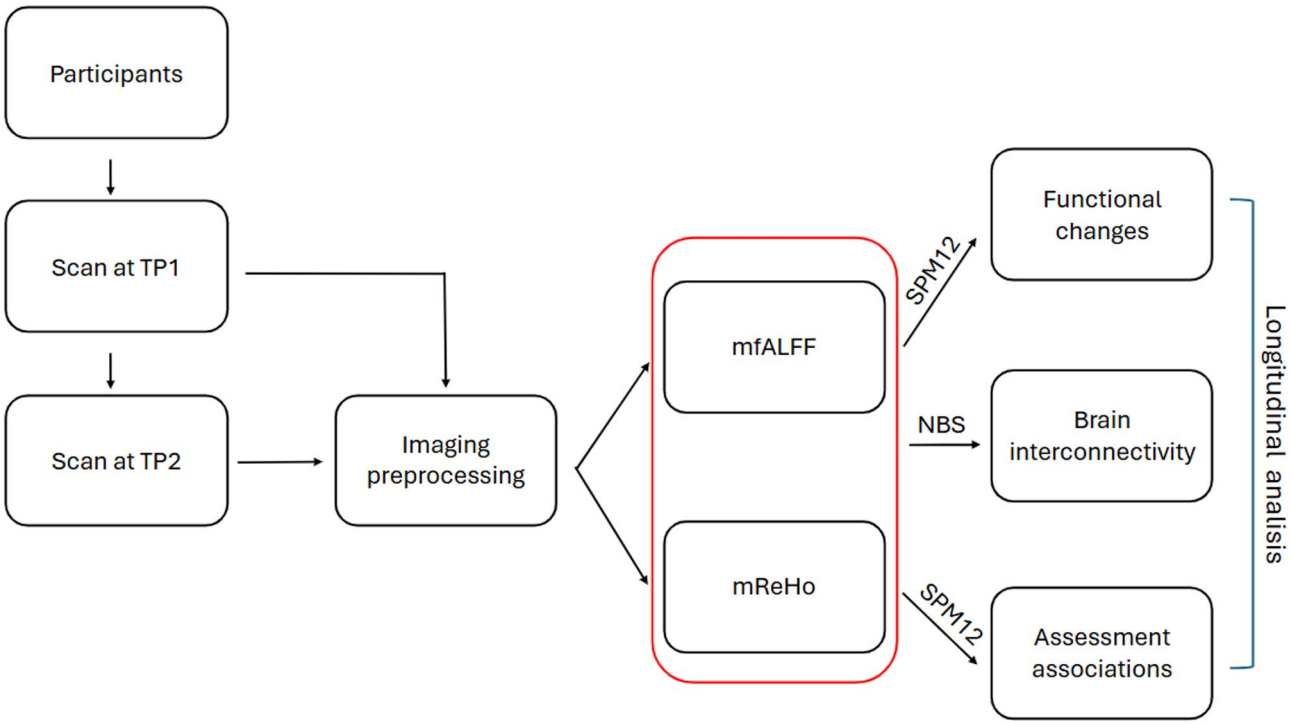


Fig. 8. The methodological pipeline.

Materials and methods

Participants

In this study, we recruited 83 subjects from Chiayi Chang Gung Memorial Hospital. The participants were divided into four groups: 25 HCs, 27 depressed patients with NS, 18 depressed patients with SI, and 13 depressed patients with SI converted to NS (improved). At the TP1 assessment, our subjects were interviewed for inclusion/exclusion criteria, and if eligible to participate in the study, they completed questionnaires assessing psychopathology and a resting-state fMRI scan. Participants returned to the hospital approximately one year (TP2) later to complete clinical assessments and a second resting-state scan. The methodological pipeline was shown in Fig. 8 to more clearly demonstrate the idea and research structure.

All participants were at least 20 years of age and right-handed. Depressive disorders and SI were primarily diagnosed by psychiatrists and indicated by scores on the Hamilton Rating Scale for Depression (HAM-D), Mini International Neuropsychiatric Interview (MINI) and Beck Scale for Suicide Ideation (BSS), which were administered by trained research nurses at both TP1 and TP2. The use of the MINI and BSS to assess SI was previously validated[25]. If either of the two assessments indicates that the patient has suicidal ideation, the patient is considered to have suicidal ideation. In the MINI, individuals were considered to have suicidal ideation if they responded "yes" to any of the first four items in the suicidality section. For BSS, if either of the following responses was given—"I have a weak wish to die" or "I somewhat want to commit suicide"—the individual was considered to have suicidal ideation. If neither scale indicates suicidal ideation, the patient is considered not to have suicidal ideation. Participants in the NS group had neither current nor past suicidal ideation and no history of suicide attempts. All the follow-up patients received similar antidepressants during the follow-up period. The control group encompassed those without depression and any antidepressant use. To minimize the influence of antidepressant use, we recruited depression cases with regular follow-up at the outpatient department and consistent antidepressant prescriptions, as documented in the medical chart records. The final confirmation was carried out by the principal investigator according to all available information. The participants were recruited from the outpatient clinic of the Department of Psychiatry at Chiayi Chang Gung Hospital via advertisements. The exclusion criteria for participants were as follows: a history of suicide attempts, another severe primary mental disorder (e.g., schizophrenia or bipolar disorder), alcohol/illicit substance use disorder during the past year, any neurological illnesses, or metallic implants or other contraindications for MRI. The Institutional Review Board of Chang Gung Memorial Hospital, Chiayi, Taiwan, approved the study (nos. 104-0838B, 104-9337B, 201602027B0). All participants provided written informed consent, and all the research was performed in accordance with relevant guidelines and regulations.

Clinical assessments

We administered four clinical assessments, including the Hamilton Depression Rating Scale (HAM-D), Hospital Anxiety and Depression Scale (HADS), Beck Scale for Suicide Ideation (BSS), and Ruminative Responses Scale (RRS). These scales were used to assess possible anxiety and depression symptoms and were administered by a trained research nurse.

Hamilton rating scale for depression (HAM-D)

The HAM-D, which was developed by M. Hamilton in 1960, is commonly used to assess depressive symptoms worldwide[26]. It is used to rate the severity of depression by probing mood, feelings of guilt, SI, insomnia, agitation or retardation, anxiety, weight loss, and somatic symptoms. A higher score indicates more severe depressive symptoms.

Hospital anxiety and depression scale- anxiety scale (HADS-A)

The HADS is a self-report scale used to assess the severity of anxiety and depressive symptoms[27]. We selected only the HADS-A in our research because we have already used the HAM-D for depression assessment. The anxiety subscale of the HADS (HADS-A) focuses on anxiety symptoms. It typically consists of 7 or 14 items. Patients are asked to report the severity of their anxiety symptoms over a specified period, usually the past week. The questions are designed to assess symptoms such as restlessness, tension, and worry. The higher the score is, the more severe the anxiety symptoms. We included an anxiety assessment since several studies have indicated that anxiety is accompanied by depression.

Beck scale for suicide ideation (BSS) score

The BSS involves self-reported data collected during a semistructured interview to assess SI. The scale was developed for adult psychiatric patients and quantifies the intensity of SI[28]. The scale contains 19 items that are divided into three categories: active suicidal desire, preparation, and passive suicidal desire. The initial findings showed promising reliability and validity. The measured content included various dimensions of suicidal tendencies, including desire, attitudes, and plans. The first five sets were used to screen participants based on their attitudes toward life and death. Only participants assessed to have active or passive suicidal ideation were required to respond to sets 6 through 19. Sets 20 and 21 primarily aim to gather information on the frequency and severity of previous suicide attempts, providing valuable reference data. We administered this scale to subjects with SI to assess the severity of SI.

Ruminative responses scale (RRS)

Rumination is defined as repeatedly dwelling on negative thoughts and the inability to think of other things[29]. Rumination is a common thinking pattern observed in individuals with depression and is associated with the severity of depressive symptoms and an increased risk of suicide. The higher the score is, the more severe the rumination.

MRI acquisition

All participants were scanned using a 3T MRI (Verio, SIEMENS, Erlangen, Germany) scanner with a standard 8-channel head coil. A gradient-echo echo planar image (EPI) sequence was used to obtain resting-state fMR images. The phase-encoded direction was along the anterior-posterior axis. During resting-state MR image acquisition, all participants were instructed to keep their eyes closed and not to think of anything in particular. For all participants, the following sequence parameters were used: repetition time (TR)/echo time (TE) = 2000/30 ms, field of view (FOV) = 220 mm × 220 mm, matrix size = 64 × 64, in-plane resolution (pixel size) = 3.4 × 3.4 mm^2slice thickness = 4 mm, number of repetitions = 300, scan time = 10 min, and 31 axial slices aligned along AC-PCs without gaps to cover the whole cerebrum.

Mean fractional amplitude of low-frequency fluctuations (mfALFF)

In resting-state fMRI, subjects are typically asked to lie still and not engage in any specific cognitive or motor tasks while their brains are scanned. The mean fractional amplitude of low-frequency fluctuations (mfALFF) and mean regional homogeneity (mReHo) are powerful indices of brain function. The fALFF reflects spontaneous fluctuations in blood oxygen level-dependent (BOLD) fMRI signal intensity in a given brain region in the resting state. Electrophysiological studies have suggested that low-frequency oscillations are derived from spontaneous neuronal activity. The frequency is usually set at 0.01 to 0.12 Hz because values in this range are meaningful. The ALFF was computed as follows: for a specific voxel, the time series was initially transformed into the frequency domain using a fast Fourier transformation. Subsequently, the square root of the power spectrum was calculated, averaged, and standardized across a predefined frequency range, which is referred to as the ALFF for that particular voxel[30]. The ALFF is extensively applied in fMRI-based theoretical models of brain function[30,31]. mALFF values were normalized so that the analysis presented more complete data, and mean fractional ALFF (mfALFF) values were calculated using the total energy over the detectable frequency range. The mfALFF can provide a more specific measure of low-frequency oscillatory phenomena than the mALFF[32]. We selected mfALFF as it effectively captures the intensity of spontaneous neuronal activity, making it suitable for identifying regional abnormalities in psychiatric conditions such as depressive disorder.

Mean regional homogeneity (mReHo)

ReHo is a voxel-based measure of brain activity that assesses the similarity or synchronization between the time series of a given voxel and its nearest neighbor[33]. This measure is based on the hypothesis that intrinsic brain activity is manifested by clusters of voxels rather than single voxels. Kendall's coefficient of concordance (KCC) is used as an index to evaluate the similarity of the time series within a cluster of a given voxel and its nearest neighbors. To analyze ReHo, linear detrending and bandpass filtering (0.01–0.12 Hz) were performed on the time series of each voxel. ReHo requires no a priori definition of ROIs and can provide information about the local/regional activity of areas throughout the brain[33]. mReHo values have been normalized. The ReHo maps were normalized for standardization purposes by dividing them by their respective mean KCC within the mask. This normalization procedure was performed to compute mReHo. We selected mReHo because it reflects the

local synchronization of neural activity, which is essential for understanding the altered coordination of brain regions in individuals with depression and suicidal ideation.

Image preprocessing

Before functional analysis, images were preprocessed by the fMRI toolbox in Statistical Parametric Mapping 12 (SPM12, Wellcome Department of Cognitive Neurology, London, UK). The preprocessing steps were as follows: (i) Each slice of the scan time differed among subjects; thus, we performed slice timing correction to ensure that all the scans were obtained at the same time point. (ii) Although the subjects refrained from movement, head motion may have occurred; thus, head motion correction was performed. (iii) The fMRI images were normalized to 3 mm voxels and matched to the East Asian Brain template from the International Consortium for Brain Mapping (ICBM) to reduce interindividual differences in brain structure. (iv) Smoothing was performed with a Gaussian kernel (6 mm full width at half maximum; FWHM) to increase the signal-to-noise ratio. These steps ensured that voxels were mapped throughout the brain. Next, we converted the imaging data into frequency-domain imaging data. First, we removed physiological signal drift by using the Resting-State fMRI Data Analysis Toolkit (REST). We detrended the image frequency between 0.01 ~ 0.12 Hz to exclude the lower frequency (machine noise) and the higher frequency (physiological noise, such as heartbeats and respiration)[34]. Second, we used smoothed data to generate mfALFF maps and unsmoothed data to generate mReHo maps. For the mReHo calculation, smoothing was not used to increase the signal because smoothing enforces a degree of autocorrelation or synchrony among spatially proximal voxels.

Statistical analysis

The repeated-measures ANCOVA, paired-t test, and multiple regression analysis were performed in SPM12. Age, sex, and years of education were included as covariates in all analyses. A false discovery rate (FDR)-corrected p value < 0.05 indicated a statistically significant difference and was used for every analysis in the study. Our results were obtained by analyzing the original images after coregistration to the MNI template. Therefore, the resultant images have the same resolution as the MNI template, which is $1 \times 1 \times 1$ mm^3. The cluster size of each result was set to be larger than 100 voxels of MNI template. In addition, the graph theoretical analysis and network-based statistic analysis were conducted by CONN first. Then, using Graph Analysis Toolbox (GAT, Stanford University School of Medicine, Stanford, CA, USA) to detect significant differences in network topological parameters and regional network measures between TP1 and TP2 in each group, using network-based statistics (NBS, Melbourne Neuropsychiatry Centre, The University of Melbourne, and Melbourne Health, Australia) to identify any potentially connected structures formed by a carefully selected group of suprathreshold links. Age, sex, and years of education were also included as covariates. To construct a set of suprathreshold links, we computed the test statistic (corrected $p < 0.05$) for each pairwise association.

Voxel-based longitudinal analysis

In the voxel-based analysis, we used two-way repeated-measures analysis of covariance (ANCOVA) in SPM12 to detect changes in brain function between TP1 and TP2 in the improved, SI, NS, and HC groups. There were three factors in the ANCOVA model, namely, the between-group factor (subject), between-group factor (group), and within-subject factor (time). The subject factor accounted for variance due to individual differences. Because the subjects were scanned with the same parameters, the analysis was carried out with a flexible factorial design to examine the group-by-time interaction. We aimed to observe the functional differences within groups according to the time interval. After repeated-measures ANCOVA, we used post hoc paired-sample t tests to determine the differences in brain function between TP1 and TP2 in the HC, NS, SI, and improved groups.

Network-based analysis: graph theoretical analysis

For network-based analysis, we used the CONN toolbox (functional connectivity toolbox, The Gabrieli Lab, McGovern Institute for Brain Research, MIT, Cambridge, MA, USA) to establish the brain network. It was divided into 90 regions of interest (ROIs) excluding the cerebellum, and each node corresponded to the automated anatomical labeling (AAL) template. Edges in the brain network represent the connectivity between two nodes. The degree of nodes reflects the number of edges connecting the node to the residual network. In other words, this map shows the distribution of nodes and edges in the brain network. The rs-MR images were registered in T1-weighted images and then normalized to the Montreal Neurological Institute (MNI) space. The transformation from the native space to the MNI space was performed with transformation matrices created in the two previously registered processing steps. We used the Graph Analysis Toolbox (GAT, Stanford University School of Medicine, Stanford, CA, USA) to investigate the network properties of the brain[35]. Specifically, the GAT was used to extract the functional connectivity among 90 regions of interest (ROIs) in each individual 90×90 connectivity matrix. Before conducting statistical analysis, it is necessary to determine the network density range in which the network is more meaningful (i.e., the density range in which the network does not break)[35]. After examining all topological parameters, we created curves of topological parameters vs. network density for each group at the same thresholds, ranging from 0.01 to 0.6 (in 0.01 increments), and identified the minimum network density (0.05) and the maximum network density (0.55) at which no individual network was fragmented, or the topological parameters exhibit no discontinuous changes. We then conducted graph theoretical analysis to examine the systematic alterations in whole-brain functional topological organization between two time points, computing various measures, such as the clustering coefficient, transitivity, global efficiency, and small-worldness index. We investigated whether there was decreased local segregation and increased global integration after treatment according to depression therapy research via graph theoretical analysis[36]. To detect significant differences in network topological parameters and regional network measures

between TP1 and TP2 in each group, the area under the curve of topological parameters vs. network density between 0.05 and 0.55 of the density was extracted to calculate the p value with a paired sample t test.

Network-based statistic analysis

We utilized network-based statistics (NBS, Melbourne Neuropsychiatry Centre, The University of Melbourne, and Melbourne Health, Australia) to detect any connected subnetworks within the altered functional connectivity networks identified over time in the HC, SI, and NS groups[37]. Network-based statistic analysis aims to identify any potentially connected structures formed by a carefully selected group of suprathreshold links. We divided the 90 brain regions according to the MNI mask. We hypothesize that there are any psychologic-related networks, e.g., the SN, default mode network (DMN), and central executive network (CEN), in our research. The significance of any such structure is determined by its topological extent.

Multiple regression

In the longitudinal study, we examined the relationships across two distinct time points within each group. Our objective was to ascertain whether the correlations underwent significant changes from TP1 to TP2 within each respective group. Multiple regression analysis is a statistical technique used to examine the relationship between a single dependent variable and several independent variables. In our study, multiple regression was used to analyze the longitudinal associations between brain function alterations (ΔmfALFF and ΔmReHo) and clinical assessment changes, including ΔHAMD, ΔHADS-A, ΔBBS, and ΔRRS scores, in each group (Δ = TP2–TP1). First, the differences (TP2–TP1) in functional mappings and assessment scores were calculated in MATLAB. Second, a general linear model (GLM) was constructed in SPM12 to detect associations between these brain function alterations and clinical assessment changes from TP1 to TP2. For example, when a result presented a negative correlation, the disease improved, but brain function also increased. In addition, scatter plots were generated to calculate the correlation coefficient.

Data availability

The data that support the findings of this study are available from the corresponding author upon reasonable request.

Received: 11 April 2025; Accepted: 2 July 2025
Published online: 09 July 2025

References

1. Organization, W. H. *Depressive Disorder (Depression)*. (World Health Organization, 2023).
2. Woody, C. A., Ferrari, A. J., Siskind, D. J., Whiteford, H. A. & Harris, M. G. A systematic review and meta-regression of the prevalence and incidence of perinatal depression. *J. Affect. Disord.* **219**, 86–92. https://doi.org/10.1016/j.jad.2017.05.003 (2017).
3. Sveticic, J. & De Leo, D. The hypothesis of a continuum in suicidality: a discussion on its validity and practical implications. *Mental Illn.* **4**, e15. https://doi.org/10.4081/mi.2012.e15 (2012).
4. Nock, M. K. et al. Cross-national prevalence and risk factors for suicidal ideation, plans and attempts. *Br. J. Psychiatry J. Ment. Sci.* **192**, 98–105. https://doi.org/10.1192/bjp.bp.107.040113 (2008).
5. Lee, S. et al. Lifetime prevalence and inter-cohort variation in DSM-IV disorders in metropolitan China. *Psychol. Med.* **37**, 61–71. https://doi.org/10.1017/s0033291706008993 (2007).
6. Nock, M. et al. (ed, K.) Cross-national analysis of the associations among mental disorders and suicidal behavior: findings from the WHO world mental health surveys. *PLoS Med.* **6** e1000123. https://doi.org/10.1371/journal.pmed.1000123 (2009).
7. Zhang, Z. J. et al. Platelet 5-HT(1A) receptor correlates with major depressive disorder in drug-free patients. *Prog. Neuro-psychopharmacol. Biol. Psychiatry*. **53**, 74–79. https://doi.org/10.1016/j.pnpbp.2014.03.004 (2014).
8. Wei, S. et al. Amygdala functional connectivity in female patients with major depressive disorder with and without suicidal ideation. *Ann. Gen. Psychiatry*. **17**, 37. https://doi.org/10.1186/s12991-018-0208-0 (2018).
9. Schwartz, J., Ordaz, S. J., Ho, T. C. & Gotlib, I. H. Longitudinal decreases in suicidal ideation are associated with increases in salience network coherence in depressed adolescents. *J. Affect. Disord.* **245**, 545–552. https://doi.org/10.1016/j.jad.2018.11.009 (2019).
10. Jalbrzikowski, M. et al. Development of white matter microstructure and intrinsic functional connectivity between the amygdala and ventromedial prefrontal cortex: associations with anxiety and depression. *Biol. Psychiatry*. **82**, 511–521. https://doi.org/10.1016/j.biopsych.2017.01.008 (2017).
11. Strikwerda-Brown, C. et al. Mapping the relationship between subgenual cingulate cortex functional connectivity and depressive symptoms across adolescence. *Soc. Cognit. Affect. Neurosci.* **10**, 961–968. https://doi.org/10.1093/scan/nsu143 (2015).
12. Chen, V. C. et al. Resting-State functional connectivity and brain network abnormalities in depressive patients with suicidal ideation. *Brain Topogr.* **34**, 234–244. https://doi.org/10.1007/s10548-020-00817-x (2021).
13. Buckner, R. L., Andrews-Hanna, J. R. & Schacter, D. L. The brain's default network: anatomy, function, and relevance to disease. *Ann. N. Y. Acad. Sci.* **1124**, 1–38. https://doi.org/10.1196/annals.1440.011 (2008).
14. Kang, L. et al. Functional connectivity between the thalamus and the primary somatosensory cortex in major depressive disorder: a resting-state fMRI study. *BMC Psychiatry*. **18**, 339. https://doi.org/10.1186/s12888-018-1913-6 (2018).
15. Huang, L. et al. Amplitude of low-frequency fluctuation (ALFF) alterations in adults with subthreshold depression after physical exercise: A resting-state fMRI study. *J. Affect. Disord.* **295**, 1057–1065. https://doi.org/10.1016/j.jad.2021.08.094 (2021).
16. Luo, Q. et al. Altered regional brain activity and functional connectivity patterns in major depressive disorder: A function of childhood trauma or diagnosis? *J. Psychiatr. Res.* **147**, 237–247. https://doi.org/10.1016/j.jpsychires.2022.01.038 (2022).
17. Yunusova, Y. et al. Frontal anatomical correlates of cognitive and speech motor deficits in amyotrophic lateral sclerosis. *Behav. Neurol.* **2019**, 9518309. https://doi.org/10.1155/2019/9518309 (2019).
18. Rehman, A. & Al Khalili, Y. In *StatPearls (StatPearls Publishing Copyright © 2024)* (StatPearls Publishing LLC., 2024).
19. Holzschneider, K. & Mulert, C. Neuroimaging in anxiety disorders. *Dialog. Clin. Neurosci.* **13**, 453–461. https://doi.org/10.31887/DCNS.2011.13.4/kholzschneider (2011).
20. Martin, E. I., Ressler, K. J., Binder, E. & Nemeroff, C. B. The neurobiology of anxiety disorders: brain imaging, genetics, and psychoneuroendocrinology. *Psychiatr. Clin. N. Am.* **32**, 549–575. https://doi.org/10.1016/j.psc.2009.05.004 (2009).
21. Cooney, R. E., Joormann, J., Eugène, F., Dennis, E. L. & Gotlib, I. H. Neural correlates of rumination in depression. *Cogn. Affect. Behav. Neurosci.* **10**, 470–478. https://doi.org/10.3758/cabn.10.4.470 (2010).

22. Li, X. et al. Alteration of whole brain alff/falff and degree centrality in adolescents with depression and suicidal ideation after electroconvulsive therapy: A Resting-State fMRI study. *Front. Hum. Neurosci.* 15–2021. https://doi.org/10.3389/fnhum.2021.762343 (2021).
23. Palmer, S. M., Crewther, S. G., Carey, L. M. & &, T. S. P. T. A Meta-Analysis of changes in brain activity in clinical depression. *Front. Hum. Neurosci.* 8-2014. https://doi.org/10.3389/fnhum.2014.01045 (2015).
24. Vieira, R., Faria, A. R., Ribeiro, D., Picó-Pérez, M. & Bessa, J. M. Structural and functional brain correlates of suicidal ideation and behaviors in depression: A scoping review of MRI studies. *Prog. Neuro-psychopharmacol. Biol. Psychiatry*. **126**, 110799. https://doi.org/10.1016/j.pnpbp.2023.110799 (2023).
25. Roaldset, J. O., Linaker, O. M. & Bjørkly, S. Predictive validity of the MINI suicidal scale for self-harm in acute psychiatry: a prospective study of the first year after discharge. *Arch. Suicide Res.* **16**, 287–302. https://doi.org/10.1080/13811118.2013.722052 (2012).
26. Zimmerman, M., Martinez, J. H., Young, D., Chelminski, I. & Dalrymple, K. Severity classification on the Hamilton depression rating scale. *J. Affect. Disord.* **150**, 384–388. https://doi.org/10.1016/j.jad.2013.04.028 (2013).
27. Annunziata, M. A. et al. Hospital anxiety and depression scale (HADS) accuracy in cancer patients. *Support. Care Cancer*. **28**, 3921 (2020).
28. Kliem, S., Lohmann, A., Mößle, T. & Brähler, E. German Beck scale for suicide ideation (BSS): psychometric properties from a representative population survey. *BMC Psychiatry*. **17**, 389. https://doi.org/10.1186/s12888-017-1559-9 (2017).
29. Parola, N. et al. Psychometric properties of the ruminative response Scale-short form in a clinical sample of patients with major depressive disorder. *Patient Prefer. Adherence*. **11**, 929–937. https://doi.org/10.2147/ppa.S125730 (2017).
30. Yue, Y., Jia, X., Hou, Z., Zang, Y. & Yuan, Y. Frequency-dependent amplitude alterations of resting-state spontaneous fluctuations in late-onset depression. *Biomed. Res. Int.* **2015**, 505479. https://doi.org/10.1155/2015/505479 (2015).
31. Wang, P. et al. Amplitude of low-frequency fluctuation (ALFF) May be associated with cognitive impairment in schizophrenia: a correlation study. *BMC Psychiatry*. **19**, 30. https://doi.org/10.1186/s12888-018-1992-4 (2019).
32. Zou, Q. H. et al. An improved approach to detection of amplitude of low-frequency fluctuation (ALFF) for resting-state fMRI: fractional ALFF. *J. Neurosci. Methods*. **172**, 137–141. https://doi.org/10.1016/j.jneumeth.2008.04.012 (2008).
33. Zang, Y., Jiang, T., Lu, Y., He, Y. & Tian, L. Regional homogeneity approach to fMRI data analysis. *Neuroimage*. **22**, 394–400. https://doi.org/10.1016/j.neuroimage.2003.12.030 (2004).
34. Baria, A. T., Baliki, M. N., Parrish, T. & Apkarian, A. V. Anatomical and functional assemblies of brain BOLD oscillations. *J. Neurosci.* **31**, 7910–7919. https://doi.org/10.1523/JNEUROSCI.1296-11.2011 (2011).
35. Hosseini, S. M. H., Hoeft, F. & Kesler, S. R. GAT: A Graph-Theoretical analysis toolbox for analyzing Between-Group differences in Large-Scale structural and functional brain networks. *PLOS ONE*. **7**, e40709. https://doi.org/10.1371/journal.pone.0040709 (2012).
36. Daws, R. E. et al. Increased global integration in the brain after psilocybin therapy for depression. *Nat. Med.* **28**, 844–851. https://doi.org/10.1038/s41591-022-01744-z (2022).
37. Zalesky, A., Fornito, A. & Bullmore, E. T. Network-based statistic: identifying differences in brain networks. *Neuroimage*. **53**, 1197–1207. https://doi.org/10.1016/j.neuroimage.2010.06.041 (2010).

Acknowledgements

This study was supported by research grants MOST109-2314-B-182-047-MY3 and NSTC112-2221-E-182-013-MY3 from the National Science and Technology Council, Taipei, Taiwan. This study was also supported by grant NMRPD1N0291~3 from Chang Gung University, Taoyuan, Taiwan. The funders of the study had no role in the study design, data collection, data analysis, data interpretation, or writing of the report.

Author contributions

J.-C.W. supervised the project. J.-C.W., V.C.-H.C., Z.-Y.Q., Y.-H.T. and G.L. contributed to the design and implementation of the research. Z.-Y.Q. analyzed the data and prepared all figures. V.C.-H.C. and Z.-Y.Q. wrote the main manuscript text. All authors contributed to the final version of the manuscript.

Declarations

Competing interests

The authors declare no competing interests.

Additional information

Supplementary Information The online version contains supplementary material available at https://doi.org/10.1038/s41598-025-10161-4.

Correspondence and requests for materials should be addressed to J.-C.W.

Reprints and permissions information is available at www.nature.com/reprints.

Publisher's note Springer Nature remains neutral with regard to jurisdictional claims in published maps and institutional affiliations.

Open Access This article is licensed under a Creative Commons Attribution-NonCommercial-NoDerivatives 4.0 International License, which permits any non-commercial use, sharing, distribution and reproduction in any medium or format, as long as you give appropriate credit to the original author(s) and the source, provide a link to the Creative Commons licence, and indicate if you modified the licensed material. You do not have permission under this licence to share adapted material derived from this article or parts of it. The images or other third party material in this article are included in the article's Creative Commons licence, unless indicated otherwise in a credit line to the material. If material is not included in the article's Creative Commons licence and your intended use is not permitted by statutory regulation or exceeds the permitted use, you will need to obtain permission directly from the copyright holder. To view a copy of this licence, visit http://creativecommons.org/licenses/by-nc-nd/4.0/.

© The Author(s) 2025